

# Surface Classification Using Conformal Structures

Xianfeng Gu

Department of CISE  
University of Florida  
Gainesville, FL 32611  
gu@cise.ufl.edu

Shing-Tung Yau

Department of Mathematics  
Harvard University  
Cambridge, MA 02138  
yau@math.harvard.edu

## Abstract

*3D surface classification is a fundamental problem in computer vision and computational geometry. Surfaces can be classified by different transformation groups. Traditional classification methods mainly use topological transformation groups and Euclidean transformation groups. This paper introduces a novel method to classify surfaces by conformal transformation groups. Conformal equivalent class is finer than topological equivalent class and coarser than isometric equivalent class, making it suitable for practical classification purposes. For general surfaces, the gradient fields of conformal maps form a vector space, which has a natural structure invariant under conformal transformations. We present an algorithm to compute this conformal structure, which can be represented as matrices, and use it to classify surfaces. The result is intrinsic to the geometry, invariant to triangulation and insensitive to resolution. To the best of our knowledge, this is the first paper to classify surfaces with arbitrary topologies by global conformal invariants. The method introduced here can also be used for surface matching problems.*

## 1. Introduction

3D surface classification and matching are fundamental problems in computer vision and computational geometry. Recent developments in modeling and digitizing techniques have led to an increasing accumulation of 3D models. This has highlighted the need for an efficient 3D object searching technique in a data set.

Many methods have been developed based on the topological and geometric features of the surfaces in order to describe shapes. In general, all the methods treat the surface as a 2D manifold with a metric structure embedded in  $R^3$ .

In this paper, we view the surfaces from a completely novel viewpoint: treating them as Riemann surfaces with conformal structures. A Riemann surface is a surface covered by holomorphic coordinate charts. The conformal

structure can be represented as matrices and is invariant under conformal transformations.

Compared to other surface classification methods, conformal classification has some advantages. It has a sound theoretical basis. Conformal equivalent classes are much finer than the topological equivalent classes and much coarser than the isometric classes. The conformal structures are intrinsic to the geometry, independent of triangulation, insensitive to resolution and local features, and robust to noises. Also, conformal invariants are concise and efficient to compute, and can be used as search keys conveniently. Hence conformal classification is more suitable for practical surface classification problems.

Conformal invariants can also be used for general surface matching problems. For many surface matching problems based on geometric features, conformal invariants can offer sufficient information to differentiate the different surfaces.

To the best of our knowledge, although conformal structure is well known, we are the first group to systematically use it for surface classification problems.

We introduce previous work and the theoretic background in the following part of this section, followed by detailed explanation of the algorithms in Section 2. Our surface classification method is introduced in Section 3. Experimental results are reported in Section 4. Finally, a brief summary and conclusion appears in Section 5, followed by a discussion of topics for future work in Section 6.

### 1.1 Previous work

3D shape classification and recognition is a core problem in computer vision. Due to its difficult boundary parameterization and high dimension, 2D shape classification methods can not be easily extended to 3D shape classification problems. To develop a 3D shape classification method, which makes use of 3D object topological and geometric features that is independent of tessellation and resolution, becomes desirable. Roughly, the current 3D shape classification methods fall into the following categories.

1. *Statistical properties based methods.* The simplest approach represents objects with feature vectors in a multidimensional space where the axes encode global geometric properties. Ankerst et al. [?] proposed shape histogram decomposing shells and sectors around a model's centroid. Osada et al. [?] represented shapes with probability distributions of geometric properties computed for points randomly sampled on an object's surface. However, these statistical methods are not discriminating enough to make subtle distinctions between shapes.
2. *Topology based methods.* Hilaga et al. [?] computed 3D shape similarity by comparing Multiresolutional Reeb Graphs(MRGs) which encodes the skeletal and topological structure at various levels of resolution. The MRG is constructed using a continuous function on the 3D shape, preferably a function of geodesic distance. These methods can not describe the geometric distinctions.
3. *Geometry based methods.* Novotni et al. [?] describe a method based on calculating a volumetric error between one object and a sequence of offset hulls of the other object. Tangelder et al. [?] represent the 3D shape by a signature representing a weighted point set. A shape similarity measurement based on weight transportation is used to compute the similarity between two shapes. Funkhouser et al. [?] developed a 3D matching algorithm that uses spherical harmonics to compute discriminating similarity measures. Kazhdan et al.[?] introduced a reflective symmetry descriptor that represents a measure of reflective symmetry for an arbitrary 3D model for all planes through the model's center of mass. These methods take into account of the embedding of the geometric shapes. The shape descriptors are respented as functions, inconvenient for searching. The classifications are too restrictive also.

## 1.2 Theoretic background

The algorithms introduced in this paper are based on the theories of Riemann surfaces, especially the holomorphic one-forms and period matrices as introduced in [?, ?]. We treat surfaces as Riemann surfaces, and compute their conformal structures.

A *conformal map* is a map which only scales the first fundamental form, hence preserving angles. If a mapping  $f : M_1 \rightarrow M_2$  is conformal, where  $M_1$  and  $M_2$  are two surfaces, suppose  $(u^1, u^2)$  are local parameters and the first fundamental form of  $M_1$  is  $ds^2 = \sum_{ij} g_{ij} du^i du^j$ , then the first fundamental form on  $M_2$  induced by  $f$  is

$$f^* g_{ij}(u^1, u^2) = \lambda(u^1, u^2) g_{ij}(u^1, u^2). \quad (1)$$

Figure 1 illustrates a conformal map from a female face surface to a square. All the rights angles on the texture are preserved on the surface, which is shown in (c) and (d).

Two surfaces are called *conformal equivalent* if there exists a conformal bijection between them. Conformal equivalent surfaces share the same *conformal invariants*, which can be represented as a matrix.

Figure 2 shows two genus one surfaces. Although they are topologically equivalent, they are not conformally equivalent. Each torus can be cut open and conformally mapped to a planar parallelogram. The shape of this parallelogram indicates the conformal equivalent class. We use the acute angle (right angle in this case) of the parallelogram and the length ratio between the two adjacent edges to represent the conformal invariants of the genus one surfaces, we call them *shape factors*. From (b) and (d), it is clear that the two tori have different shape factors. Hence conformal classification is finer than topological classification.

For higher genus surfaces, the conformal invariants are more complicated. Basically, each handle of the surface can be cut open and conformally mapped to a parallelogram with different shapes. Figure 4 demonstrates a genus three surface, where each handle is conformally mapped to a parallelogram. The shapes of the three parallelograms are the conformal invariants. The rigorous representation of conformal invariants of a high genus surface, through *period matrices*, is explained below.

If a surface is mapped to the complex plane, and the mapping is conformal everywhere on the surface, then we call the complex gradient vector field of the mapping a *holomorphic 1-form*. All the holomorphic 1-forms on the surface form a real vector space, which we call *holomorphic differentials*. The dimension of the holomorphic differentials is equal to two times the number of genus.

All the closed curves on the surface form a group in the sense that they can be duplicated, merged and split. Two closed curves are *homologous equivalent* if they together bound a 2D surface patch. The group of all the homologous equivalent classes is called the *homology group*.

Let  $M$  be a closed surface of genus  $g$ , and  $B = \{e_1, e_2, \dots, e_{2g}\}$  be an arbitrary basis of its homology group. We define the entries of the *intersection matrix*  $C$  of  $B$  as

$$c_{ij} = -e_i \cdot e_j \quad (2)$$

where the dot denotes the number of intersections, counting +1 when the direction of the cross product of the tangent vectors of  $e_i$  and  $e_j$  at the intersection point is consistent with the normal direction, -1 otherwise.

A holomorphic basis  $B^* = \{\omega_1, \omega_2, \dots, \omega_{2g}\}$  is defined to be dual of  $B$  if

$$Re \int_{e_i} \omega_j = c_{ij}. \quad (3)$$



(a) Original Surface (b) Conformal map to the plane (c) Checkerboard texture (d) Texture mapped surface

Figure 1: Conformal mapping. The original surface is a real human face (a), which is conformally mapped to a square (b). A checker board texture (c) is mapped back to the face. All the right angles on the texture are preserved on (d).

Define matrix  $S$  as having entries

$$Im \int_{e_i} \omega_j = s_{ij}. \quad (4)$$

The matrix  $R$  defined as

$$CR = S \quad (5)$$

satisfies  $R^2 = -I$ , where  $I$  is the identity matrix. After H.Weyl [?] and C.L.Siegel [?],  $R$  is called the *period matrix* of  $M$  with respect to the homology basis  $B$ .

The matrices  $(R, C)$  determine the conformal equivalent class of  $M$  in the following sense: For two surfaces  $M_1$  and  $M_2$  with  $(R_1, C_1)$  and  $(R_2, C_2)$  respectively,  $M_1$  and  $M_2$  are conformal equivalent if and only if there exists an integer matrix  $N$  such that

$$N^{-1}R_1N = R_2; N^T C_1 N = C_2. \quad (6)$$

We call  $(R, C)$  the *conformal structure* of  $M$ .

In the following sections, we will introduce a method to compute the shape factors for genus one surfaces, and  $(R, C)$  for higher genus surfaces, and use them to classify surfaces.

## 2 Computing Conformal Invariants

In this section, we assume inputs to our algorithm are non-zero genus triangular meshes and introduce a method to compute the holomorphic differential group and homology group. The method is improved from the algorithm introduced in [?].

Let  $K$  be a simplicial complex whose topological realization  $|K|$  is homeomorphic to a compact 2-dimensional manifold. Suppose there is a piecewise linear embedding

$$F : |K| \rightarrow R^3.$$

The pair  $(K, F)$  is called a triangular mesh and denoted as  $M$ .

### 2.1 Computing homology

Suppose  $M$  is a triangular mesh, we use  $[u, v]$ ,  $[u, v, w]$  to represent its one and two dimensional simplices. We define chain spaces as the following:

$$C_p K = \left\{ \sum \alpha_i \sigma_p^i \mid \alpha_i \in Z \right\}, p = 0, 1, 2,$$

where  $\sigma_p^i$ 's are  $p$  dimensional simplices in  $K$ . Therefore, the linear space  $C_2 K$  is the space representing all the surface patches on  $M$ ,  $C_1 K$  is the the space representing all the curves on  $M$ , and  $C_0 K$  is the space representing all the points on  $M$ . The boundary operators are linear mappings  $\partial_p : C_p K \rightarrow C_{p-1} K$ :

$$\partial_p \left( \sum_i \alpha_i \sigma_p^i \right) = \sum_i \alpha_i \partial_p \sigma_p^i, p = 1, 2.$$

The boundary operators defined on each simplex are as follows:

$$\partial_2([u, v, w]) = [u, v] + [v, w] + [w, u]$$

where  $[u, v, w]$  is a face,  $[u, v]$ ,  $[v, w]$  and  $[w, u]$  are its three edges with consistent orientation. Therefore,  $\partial_2$  is an operation that returns the boundary of a surface patch.  $\partial_1$  is defined in a similar way.  $\partial_2$  and  $\partial_1$  are linear operators and can be represented as integer matrices with elements 0, 1 or -1.

The kernel space of  $\partial_1$  is the set of all closed curves, since closed curves do not have boundaries. The image space of  $\partial_2$  is the set of all surface patch boundaries.

The homology group is defined as the quotient space in [?]

$$H_1(M, Z) = \frac{\ker \partial_1}{\text{img} \partial_2}.$$

The homology bases are the eigenvectors of the kernel space of the linear operator  $L : C_1 K \rightarrow C_1 K$ :

$$L = \partial_1^T \partial_1 + \partial_2 \partial_2^T.$$

$L$  is symmetric, the eigenvectors for the zero eigenvalue are the basis of  $H_1(M, Z)$ . Suppose  $B = \{e_1, e_2, \dots, e_{2g}\}$  is a

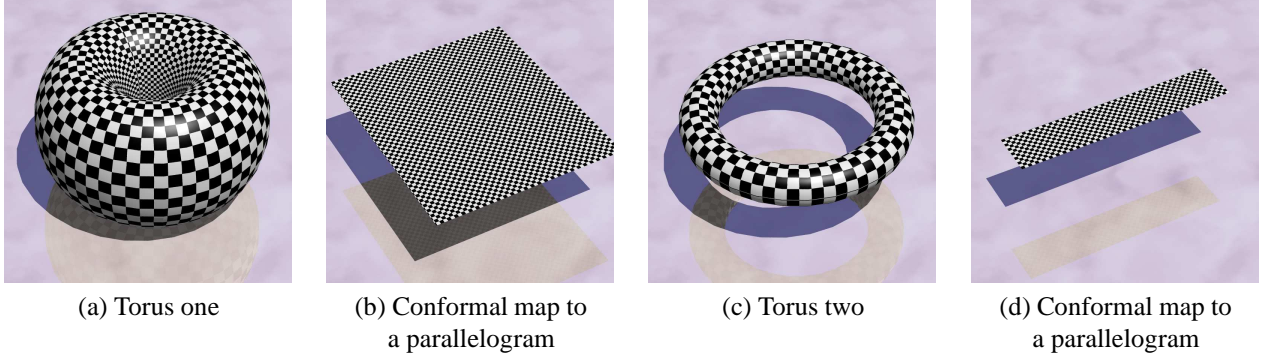


Figure 2: Topological equivalence but not conformal equivalence. The two tori (a) and (c) are topologically equivalent, but not conformally equivalent. Because they conformally map to planar parallelograms with different shapes.

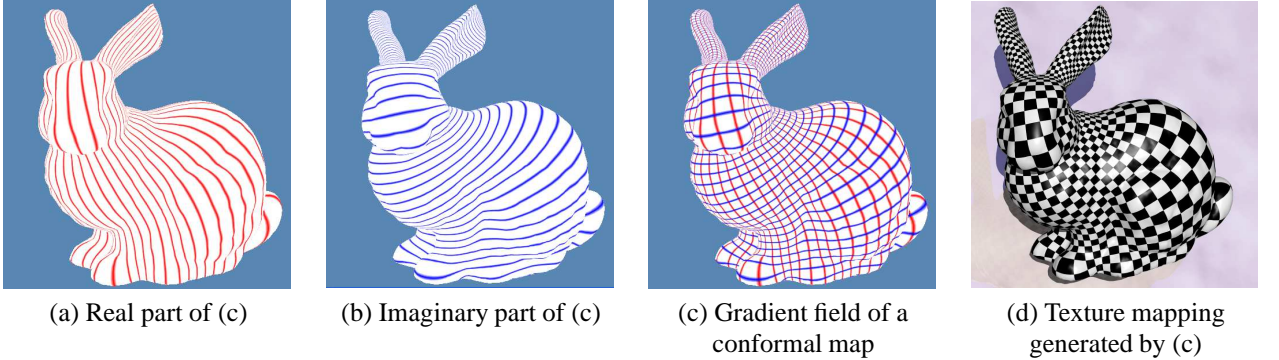


Figure 3: Holomorphic 1-form is a complex gradient field of a conformal map from the surface to the complex plane. (c) illustrates a holomorphic 1-form. (a) is the integration curves of the real part of (c), (b) is the integration curves of the imaginary part of (c). (d) visualizes the holomorphic 1-form by a texture mapping.

set of homology basis, the intersection matrix  $C$  is a skew-symmetric matrix. In order to simplify the classification process, we can make the homology basis a canonical one  $\tilde{B}$ , such that  $\tilde{B} = \{a_1, \dots, a_g, b_1, \dots, b_g\}$ ,  $a_i \cdot b_i = +1$ , and other intersection numbers are zeros. For any closed surfaces, such canonical homology basis always exists. Figure 6 illustrates such canonical homology bases for a genus 2 surface. Canonical homology basis is not unique, as shown in the figure. The intersection matrix of a canonical homology basis has a special format:

$$\tilde{C} = \begin{pmatrix} 0 & -I_g \\ I_g & 0 \end{pmatrix}, \quad (7)$$

where  $I_g$  is a  $g \times g$  identity matrix.

There exists an unitary integer matrix  $N$  (Its determinant is either 1 or -1), such that  $NCN^T = \tilde{C}$ .

Both  $C$  and  $\tilde{C}$  are congruent skew-symmetric matrices.  $C$  and  $\tilde{C}$  can be diagonalized by orthogonal matrices  $U$  and  $V$  respectively, i.e.  $C = U\Lambda U^T$  and  $\tilde{C} = V\Lambda V^T$ ,  $\Lambda = \text{diag}\{J_1, J_2, \dots, J_g\}$ ,

$$J_i = \begin{pmatrix} 0 & +1 \\ -1 & 0 \end{pmatrix}, i = 1, 2, \dots, g.$$

The  $N$  is simply  $N = VU^T$ . The canonical homology basis

can be obtained by  $\tilde{B} = BN^T$ . In the following discussion, we assume the homology bases are canonical ones.

## 2.2 Computing harmonic one-forms

We define the linear functional spaces of  $C_2K$ ,  $C_1K$  and  $C_0K$  as  $C^2K$ ,  $C^1K$  and  $C^0K$  respectively. In other words,  $C^2K$  is the set of all the linear functions defined on the surface patches,  $C^1K$  is the set of all linear functions defined on the curves on the surface. We can then define the coboundary  $\delta_1$  and  $\delta_0$  as the adjoint operator of  $\partial_2$  and  $\partial_1$ , such that

$$\delta^p \omega(\sigma) = \omega \partial_{p+1}(\sigma), p = 0, 1, \quad (8)$$

where  $\omega \in C^pK$ ,  $\sigma \in C_{p+1}K$ . Suppose  $\omega \in C^1K$ , if  $\delta^1 \omega \equiv 0$ , then  $\omega$  is called a *closed one-form*, and for any  $[u, v, w] \in K$ ,

$$\delta \omega([u, v, w]) = \omega([u, v]) + \omega([v, w]) + \omega([w, u]) = 0. \quad (9)$$

We use  $C^1K$  to represent tangential vector fields on  $M$  and associate an energy with each  $\omega \in C^1K$ :

$$E(\omega) = \frac{1}{2} \sum_{[u, v] \in K_1} k_{u, v} \|\omega([u, v])\|^2, \quad (10)$$

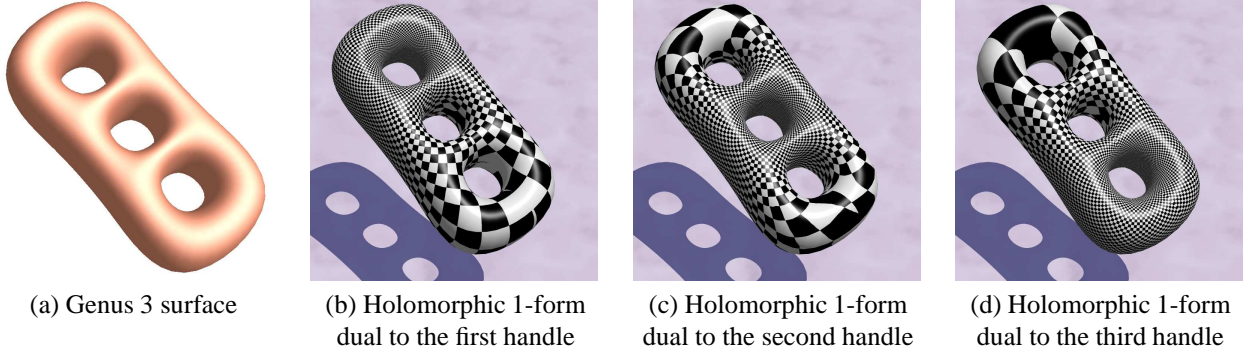


Figure 5: Holomorphic one-form basis of a genus 3 surface. Each holomorphic base is dual to one handle.

where  $k_{u,v} = \frac{1}{2}(\cot \alpha + \cot \beta)$ ,  $\alpha$  and  $\beta$  are the two angles against the edge  $[u, v]$ .  $E(\omega)$  is called the *harmonic energy* of  $\omega$ . A closed one-form which minimizes the harmonic energy is called a *harmonic one-form*. The Laplacian is a linear operator  $\Delta : C^1 K \rightarrow C^0 K$ ,

$$\Delta \omega(u) = \sum_{[u,v] \in K} k_{u,v} \omega([u, v]). \quad (11)$$

Harmonic one-forms have zero Laplacian.

According to Hodge theory [?], all the harmonic one-forms form a real linear space, which can be treated as a dual space ( linear functional space ) of the homology group  $H_1(M, Z)$ . Given a homology basis  $B = \{e_1, e_2, \dots, e_{2g}\}$ , we can compute a dual basis of the harmonic one-forms  $\{\omega_1, \omega_2, \dots, \omega_{2g}\}$  by the following linear system:

$$\begin{cases} \delta \omega_i & \equiv & 0 \\ \Delta \omega_i & \equiv & 0 \\ \int_{e_j} \omega_i & = & \delta_j^i \end{cases}, \quad (12)$$

where  $\delta_j^i$  is the Kronecker symbol. This linear system can be solved by iterative methods efficiently.

## 2.3 Computing holomorphic one-forms

Holomorphic one-forms are the gradient fields of conformal maps, which can be formulated as  $\omega + \sqrt{-1}^* \omega$ , where  $\omega$  and  $^* \omega$  are harmonic one-forms, and  $^* \omega$  is orthogonal to  $\omega$  everywhere, i.e.

$$^* \omega = n \times \omega, \quad (13)$$

$n$  is the normal field on  $M$ .  $^* \omega$  is called the conjugate harmonic one-form of  $\omega$ . In order to compute  $^* \omega$ , we construct a linear system based on the wedge product of closed one-forms. Given two closed one-forms  $\tau_1, \tau_2 \in C^1 K$ , we define the wedge product as the following linear operator  $\wedge : C^1 K \times C^1 K \rightarrow C^2 K$ ,

$$\tau_1 \wedge \tau_2([u, v, w]) = \frac{1}{6} \begin{vmatrix} \tau_1([u, v]) & \tau_1([v, w]) & \tau_1([w, u]) \\ \tau_2([u, v]) & \tau_2([v, w]) & \tau_2([w, u]) \\ 1 & 1 & 1 \end{vmatrix}. \quad (14)$$

Similarly, we can define the conjugate wedge product of  $\tau_1$  and  $\tau_2$ , denoted as  $\wedge^*$ ,

$$\tau_1 \wedge^* \tau_2(f) = u M v^T, \quad (15)$$

where  $u = (\tau_1([u, v]), \tau_1([v, w]), \tau_1([w, u]))$ ,  $v = (\tau_2([u, v]), \tau_2([v, w]), \tau_2([w, u]))$ , and

$$M = \frac{1}{24S} \begin{pmatrix} 2(l_2^2 + l_3^2) & l_1^2 + l_2^2 - l_3^2 & l_1^2 + l_3^2 - l_2^2 \\ l_1^2 + l_2^2 - l_3^2 & 2(l_3^2 + l_1^2) & l_2^2 + l_3^2 - l_1^2 \\ l_1^2 + l_3^2 - l_2^2 & l_2^2 + l_3^2 - l_1^2 & 2(l_1^2 + l_2^2) \end{pmatrix} \quad (16)$$

$|[u, v]| = l_1$ ,  $|[v, w]| = l_2$ ,  $|[w, u]| = l_3$ , and  $S$  is the area of face  $[u, v, w]$ .

Given a harmonic one-form  $\omega$ , then  $^* \omega$  is still a harmonic one-form and satisfies the following linear equations

$$\int_M \omega_i \wedge (^* \omega) = \int_M \omega_i \wedge^* \omega, i = 1, 2, \dots, 2g \quad (17)$$

where  $\omega_i$ 's are a set of basis of harmonic one-forms. Because  $^* \omega$  is still a harmonic one-form, it can be represented as a linear combination of  $\omega_i$ 's, suppose  $^* \omega = \sum_{i=1}^{2g} \alpha_i \omega_i$ , then equation (17) becomes

$$\int_M \omega_i \wedge^* \omega = \sum_{j=1}^{2g} \alpha_j \int_M \omega_i \wedge \omega_j, i = 1, 2, \dots, 2g \quad (18)$$

Given a harmonic one-form basis  $\{\omega_1, \omega_2, \dots, \omega_{2g}\}$ , we can compute the conjugate harmonic one-forms  $^* \omega_i$ 's, then  $\{\omega_i + \sqrt{-1}^* \omega_i, i = 1, 2, \dots, 2g\}$  is a basis of holomorphic one-forms.

## 2.4 Computing period matrix

For a genus one surface  $M$ , there are two homology base curves  $e_1, e_2$ . Suppose  $e_1, e_2$  only intersect at a point  $p$ . we can cut the surface open along  $e_1, e_2$ , then obtain a topological disk  $M'$ . Then we choose one vertex to map to the origin of the complex plane, and integrate the holomorphic one-form on  $M'$ . Then  $M'$  is conformally mapped to the complex plane. Point  $p$  will be mapped to four points, which



form a parallelogram. We can compute the acute angle and adjacent edge length ratio of this parallelogram, which are the conformal invariants of  $M$ .

For a higher genus surface, suppose we have computed a canonical homology basis  $\tilde{B} = \{e_1, e_2, \dots, e_{2g}\}$ , such that  $e_i \cdot e_j = \delta_j^{i+g}, 1 \leq i \leq g < j \leq 2g, \delta_j^{i+g}$  is the Kronecker symbol, and constructed a dual holomorphic differential basis  $B^* = \{\omega_1 + \sqrt{-1}^* \omega_1, \omega_2 + \sqrt{-1}^* \omega_2, \dots, \omega_{2g} + \sqrt{-1}^* \omega_{2g}\}$ , then the matrices  $C$  and  $S$  have entries:

$$c_{ij} = \int_{e_i} \omega_j, s_{ij} = \int_{e_i} {}^* \omega_j. \quad (19)$$

Then  $R$  is computed as  $R = C^{-1}S$ .  $(R, C)$  are the conformal invariants.

## 2.5 Double covering

For surfaces with boundaries, we can convert them to closed ones by the so called *double covering* technique. Given a surface  $M$  with boundaries, we make a copy of  $M$  denoted as  $M'$ , then reverse the orientation of  $M'$ . We simply glue  $M$  and  $M'$  together along their corresponding boundaries, the obtained surface  $\tilde{M}$  is a closed surface and called the *double covering* of  $M$ . We can then classify the surfaces with boundaries by the period matrices of its double covering. Figure 7 shows an example of double covering, (a) is the original genus one surface with three boundaries. (c) is its double covering, which is of genus four. (d) shows a texture mapping generated by a holomorphic one-form of the double covering.

All genus zero surfaces are conformal equivalent. It is impossible to differentiate them by their conformal structures directly. In practice, we can locate the critical points of their Gaussian curvature and remove them from the surface. The obtained surfaces are with boundaries and can be classified by using the double covering technique.

Figure 3 shows a genus zero example. Three holes are punched on the bunny surface, the bottom, and the tips of

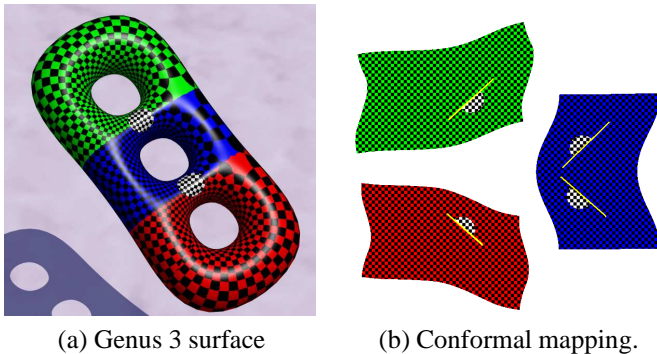


Figure 4: For higher genus surfaces, each handle can be conformally mapped to a parallelogram on the complex plane.

the ears. (d) illustrates a holomorphic one-form computed on the double covering, visualized by texture mapping a checkerboard pattern.

## 3 Surface Classification and Matching Method

Suppose  $M_1$  and  $M_2$  are two surfaces, the corresponding period matrices are  $(R_1, C_1)$  and  $(R_2, C_2)$  respectively.  $R_i$  can be decomposed as  $P_i \Lambda_i P_i^{-1}$ , where  $\Lambda_i$  is the Jordan norm form of  $R_i$ . If  $M_1$  is conformal equivalent to  $M_2$ , then

$$\Lambda_1 = \Lambda_2 \quad (20)$$

and  $N = P_1 P_2^{-1}$  is an integer matrix with determinant  $\pm 1$ . Furthermore,

$$N^T C_1 N = C_2. \quad (21)$$

Equations (20) and (21) are the sufficient and necessary conditions to verify whether two surfaces are conformal equivalent. In our case,  $C_i$ 's are canonical, matrices satisfying equation 21 are called symplectic matrices.

Then the surface classification problem is reduced to how to classify period matrices  $R$  under the integer symplectic matrix group. It has been proven that for genus  $g$  surfaces, the equivalent class of  $R$  is  $6g - 6$  dimensional [?]. We will introduce a method to compute these  $6g - 6$  parameters in our future work.

In practice, we use the sorted eigenvalues of  $R$  as the indices for surface indexing and matching.

## 4 Experiments Results

The algorithm is purely algebraic and easy to implement. The algorithm is intrinsic to the geometry, independent of triangulation and insensitive to resolution. The conformal structure is global and insensitive to local features and robust to noises. Figure 8 illustrates holomorphic one-forms, visualized by texture mapping a checkerboard image. The scaling of each texcel, and direction of iso-parametric curves are consistent under different triangulation and resolution. Comparing (a) and (c), we can see that

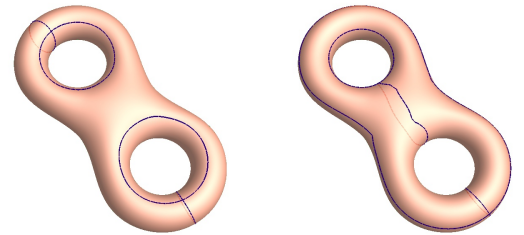


Figure 6: Canonical homology bases.

the resolutions and the triangulation are quite different. This shows the algorithm is intrinsic to the geometry and independent of the surface representation.

Table 1 shows the conformal invariants of the genus one surfaces illustrated in figure 9. By examining their shape factors, it is easy to verify that there are no two surfaces that are conformal equivalent.

mesh	angle (degree)	length ratio	vertices	faces
torus	89.987	2.2916	1089	2048
knot	85.1	31.150	5808	11616
knot2	89.9889	25.2575	2050	3672
rocker	85.432	4.9928	3750	7500
teapot	89.95	3.0264	17024	34048

Table 1: Conformal invariants of genus one surfaces.

The following are the period matrices  $R$ 's for some genus two surfaces. All the intersection matrices  $C$ 's are in the canonical form as equation (7).

The two hole torus mesh as shown in 10(a) has 861 vertices and 1536 faces. Its period matrix is

$$\begin{pmatrix} -1.475e-3 & 4.840e-4 & 4.501e-1 & 2.132e-2 \\ 4.858e-4 & -1.439e-3 & 2.132e-2 & 4.501e-1 \\ -2.260e+0 & 1.090e-1 & 1.476e-3 & -4.858e-4 \\ 1.090e-1 & -2.260e+0 & -4.840e-4 & 1.439e-3 \end{pmatrix} \quad (22)$$

The vase model shown in 10(b) has 1582 vertices and 2956 faces. Its period matrix is

$$\begin{pmatrix} 1.053e-3 & -8.838e-6 & 4.479e-1 & 2.127e-2 \\ -1.080e-4 & -1.031e-3 & 2.127e-2 & 4.042e-1 \\ 2.309e+0 & 1.241e-1 & 1.053e-3 & -1.080e-4 \\ -1.241e-1 & -2.564e+0 & 8.851e-6 & 1.031e-3 \end{pmatrix} \quad (23)$$

The flower model shown in 10(c) has 5112 vertices and 10000 faces. Its period matrix is

$$\begin{pmatrix} 6.634e-3 & -1.950e-3 & 2.861e-1 & -6.076e-2 \\ -1.909e-3 & 7.091e-3 & -6.076e-2 & 2.497e-1 \\ -3.768e+0 & -9.111e-1 & -6.634e-3 & 1.909e-3 \\ -9.111e-1 & -4.303e+0 & 1.950e-3 & -7.091e-3 \end{pmatrix} \quad (24)$$

The knotty bottle model shown in 10(d) has 15000 vertices and 30000 faces. Its period matrix is

$$\begin{pmatrix} -1.911e-2 & 2.757e-3 & 5.617e-2 & -1.001e-3 \\ 1.213e-3 & -9.294e-2 & -1.003e-3 & 5.699e-2 \\ -1.792e+1 & -4.829e-1 & 1.912e-2 & -6.224e-4 \\ -4.817e-1 & -1.819e+1 & -3.355e-3 & 9.295e-2 \end{pmatrix} \quad (25)$$

By checking the conditions of equations (20) and (21), it can be verified easily that all the surfaces above belong to different conformal equivalent classes.

We tested our algorithm on other complex models scanned from real models, the highest genus is 7 and the biggest surface is with hundreds of thousands of faces.

The computational procedure is stable. We also retriangulated several surfaces, and compared the computing results, which are very close. For example, we computed the shape factors of the teapot surfaces with different resolutions as shown in figure 8, the high resolution shape factors are (89.95, 3.0264), the low resolution shape factors are (89.98, 3.0936).

## 5. Summary and Conclusions

This paper introduces a surface classification method based on the Riemann surface theories. All surfaces can be classified by the conformal transformation group and their conformal invariants can be represented by period matrices. The method is intrinsic to the geometry, independent of triangulation and insensitive to resolution. The conformal invariants are global features of surfaces, hence they are robust to noises. The conformal equivalent classification is finer than topological classification and coarser than isometric classification, making it suitable for surface classifications and matching.

## 6 Future Work

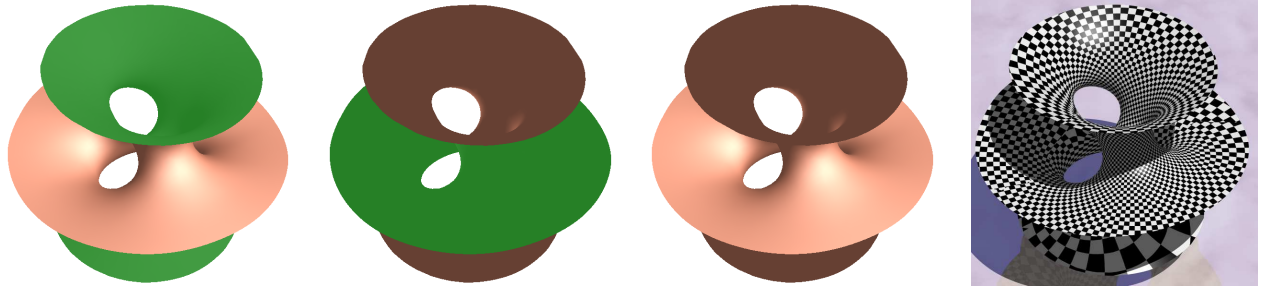
In the future, we will test our algorithm using larger scale geometric databases. We also would like to explore ways to improve efficiency in computing harmonic one-forms, which is the most time consuming step of the current process. We also would like to generalize our current algorithm to non-manifold surfaces and implicit surfaces.

## References

- [1] M. Ankerst, G. Kastenmuller, H.-P. Kriegel, and T. Seidl. 3d shape histograms for similarity search and classification in spatial databases. In *Symposium on Large Spatial Databases*, pages 207–226, 1999.
- [2] R. Osada, T. Funkhouser, B. Chazelle, and D. Dobkin. Shape distributions. *ACM Transactions on Graphics*, 21:807–832, October 2002.
- [3] M. Hilaga, Y. Shinagawa, T. Kohmura, and T.L. Kunii. Topology matching for fully automatic similarity estimation of 3d shapes. In *Proceedings of SIGGRAPH 2001*, pages 203–212, 2001.
- [4] M. Novotni and R. Klein. A geometric approach to 3d object comparison. pages 167–175, May 2001.
- [5] J.W.H. Tangelder and R.C. Veltkamp. Polyhedral model retrieval using weighted point sets. In *Proceedings of the eight annual conference of the Advanced School for Computing and Imaging*, pages 223–230, 2002.
- [6] T. Funkhouser, P. Min, M. Kazhdan, J. Chen, A. Halderman, D. Dobkin, and D. Jacobs. A search engine for 3d models. *ACM Transactions on Graphics*, 22, 2003.
- [7] M. Kazhdan, B. Chazelle, D. Dobkin, T. Funkhouser, and S. rusinkiewicz. A reflective symmetry descriptor for 3d models. *Algorithmica*, 2003.
- [8] E. Arbarello M. Cornalba P. Griffiths and J. Harris. *Topics in the Theory of Algebraic Curves*. 1938.

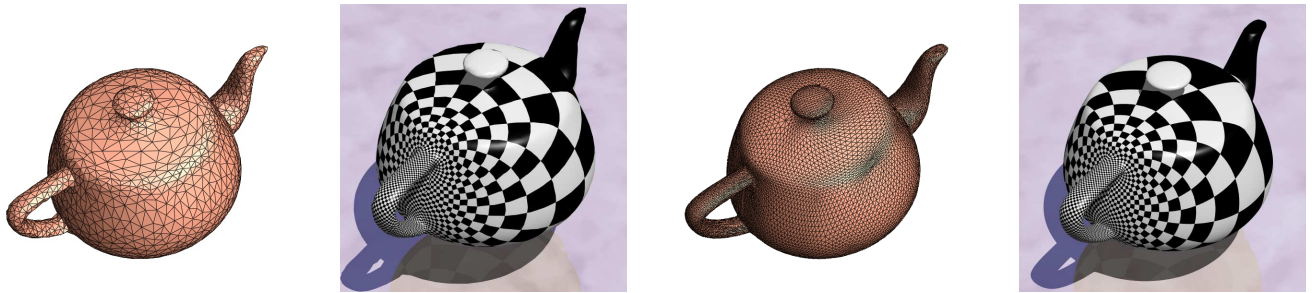
- [9] R. Schoen and S.T. Yau. *Lectures on Harmonic Maps*. International Press, Cambridge MA, 1997.
- [10] H. Weyl. On generalized riemann surfaces. *Ann. of Math.*, 35:714–725, 1934.
- [11] C.L. Siegel. Algebras of riemann matrices - tata institute of fundamental research,. *Lecture on Mathematics and Physics*, 1956.
- [12]
- [13] J.R. Munkres. *Elements of Algebraic Topology*. Addison Wesley, 1984.





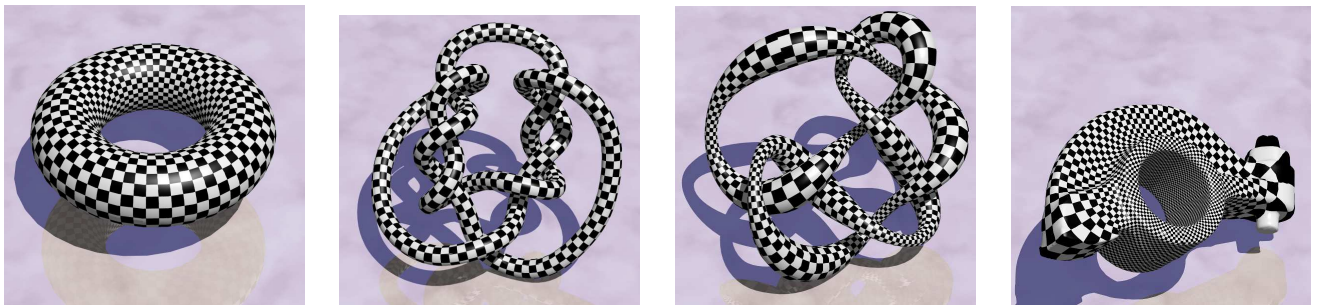
(a) Original Surface      (b) Reversed orientation      (c) Double covering      (d) Holomorphic one-form

Figure 7: Double covering. Green means the back faced part of the surface. Glue (a) and (b) along the boundaries to get (c). A holomorphic 1-form is visualized by a checkerboard texture mapping.



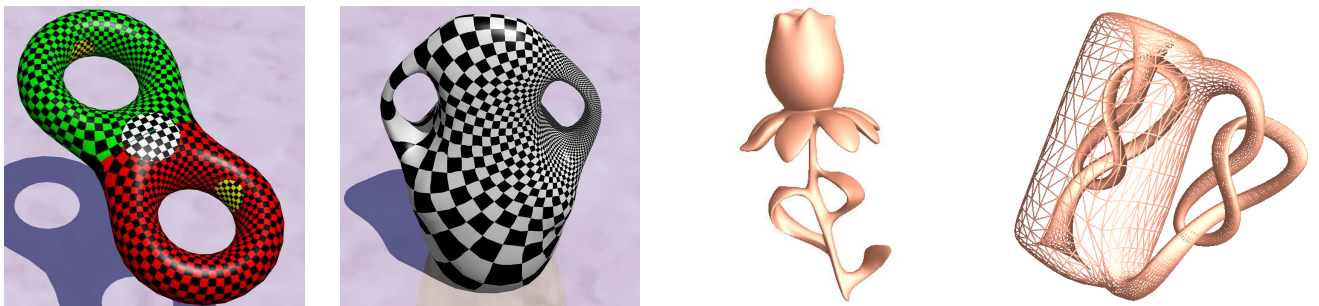
(a) Surface with 4K faces      (b) Holomorphic 1-form of (a)      (c) Surface with 34K faces      (d) Holomorphic 1-form of (c)

Figure 8: Conformal structure is only dependent on geometry, independent of triangulation and insensitive to resolution.



(a) A torus surface      (b) A knot surface (a)      (c) Another knot surface      (d) A rocker

Figure 9: Genus one surfaces with different conformal structures.



(a) A two hole torus surface      (b) A vase surface      (c) A rose surface      (d) A knotty surface

Figure 10: Genus two surfaces with different conformal structures.